

# Two-dimensional modal actuator as energy efficient design

Shailendra Joshi

Former Research Student, Department of  
Civil Engineering, Indian Institute of  
Technology Bombay, Mumbai – 400 076,  
India

Abhijit Mukherjee

Professor, Department of Civil  
Engineering, Indian Institute of  
Technology Bombay, Mumbai – 400 076,  
India

## ABSTRACT

This article demonstrates the energy consumption characteristics of a two-dimensional modal actuator. In order to obtain the modal design, a gradientless shape optimization algorithm based on residual voltages is outlined. The validity of the actuator design obtained from the design technique is established. The energy consumption characteristics of the actuator designed for the fundamental mode of a simply supported rectangular plate are studied. The modal actuator demonstrates improved response characteristics and reduced electrical energy consumption in comparison to *unweighted* actuator.

**Keywords:** Active structural control, energy efficiency, 2D modal actuator, shape optimization, gradientless algorithm

## 1. INTRODUCTION

Piezoelectric materials have gained significance as energy transducers in the real-time precise control of structures. An important application is active vibration suppression wherein these materials are employed as actuators to generate desired control forces through the conversion of electrical energy into mechanical energy. In such an application a critical issue that needs to be addressed is the electrical energy that the actuators consume in order to produce the desired mechanical response. The minimization of the energy consumption of the actuators stems from the ubiquitous desire to design efficient systems. Moreover, in many practical situations only limited power may be available. Furthermore, the knowledge of energy consumption is also necessary to design the driving electronics for the active vibration. In the present article, we investigate the energy consumption characteristics of an actuator design optimized to excite a particular vibration mode in the structure, known as *modal actuator*.

Modal sensing and actuation has been a topic of interest in recent years<sup>1</sup>. One of the ways of designing modal actuators is by shaping the electrode surface and selectively poling it such that it excites only the specific modes of interest. Modal actuators combined with modal sensors improve the control characteristics as they minimize the spillover effects

and alleviate the need for exhaustive signal processing<sup>2</sup>. Lee and Moon<sup>3</sup> developed a theory to derive modal sensors and actuators for one-dimensional structures using modal equations. Friswell<sup>4</sup> used finite element shape functions to design modal sensors and actuators for Euler-Bernoulli beams. Mukherjee and Joshi<sup>5</sup> presented a gradientless shape design procedure to obtain spatially optimized transducers for shape control of piezolaminated plates.

Few researchers have addressed the issue of power and energy consumption of piezoelectric actuators in exciting the structures<sup>6-9</sup>. Mukherjee and Joshi<sup>10</sup> presented an iterative technique to determine actuator profiles that minimize power consumption in obtaining the desired displacements in the structure. The authors investigated the energy efficiency of a one-dimensional modal actuator under dynamic conditions<sup>11</sup>. In this paper, we extend the concept to two dimensional modal actuator designs. A simply supported rectangular plate is considered as a demonstration model and the mode-1 actuator is employed in controlling the response of the plate. The modal actuator design is obtained using the gradientless design algorithm developed by the authors<sup>5</sup>. The response of the modal actuator is compared with that of the unweighted actuator. It is found that the modal actuator is more energy efficient than the unweighted actuator.

## 2. MATHEMATICAL FORMULATION

The equations of motion for a structure subjected to time-dependent forces can be written as a set of second order differential equations in the following form,

$$\mathbf{M}\ddot{\mathbf{d}} + \mathbf{C}\dot{\mathbf{d}} + \mathbf{K}\mathbf{d} = \mathbf{F}(\mathbf{t}) \quad (1)$$

Where,  $\mathbf{M}$ ,  $\mathbf{C}$  and  $\mathbf{K}$  are the mass, damping and stiffness matrices of the system,  $\ddot{\mathbf{d}}$ ,  $\dot{\mathbf{d}}$  and  $\mathbf{d}$  are the acceleration, velocity and displacement vectors. The force vector  $\mathbf{F}(\mathbf{t})$  comprises of the vectorial sum of external time-dependent forces and the control forces. In the present work, an eight-node plate finite element with five degrees of freedom per node ( $u$ ,  $v$ ,  $w$ ,  $\mathbf{q}_x$  and  $\mathbf{q}_y$ ) is employed. The detailed formulation

for the mass, stiffness and the damping matrices can be found elsewhere<sup>13</sup>. A brief explanation on the formulation of the force vector is presented here.

### 2.1 Force vector

The force vector comprises of two parts; viz. the externally applied time-dependent forces and the time-dependent actuator forces generated by the piezoelectric actuators. The sensors in the system sense the signal due to externally applied forces. The signal is fed back to the actuator that generates the control forces. In this section, the formulation of the sensor and actuator mechanics is discussed in brief.

#### SENSOR MECHANICS

The equation governing the sensor mechanics is as follows,

$$\mathbf{D}^k = \mathbf{e}^k \mathbf{e}^k + \bar{\mathbf{e}}^k \mathbf{E}^k \quad (2)$$

Where,  $\mathbf{D}^k$  corresponds to the electric field displacement vector,  $\mathbf{e}^k$  is the matrix of piezoelectric constants,  $\mathbf{e}^k$  is the strain vector,  $\bar{\mathbf{e}}^k$  is the matrix of dielectric constants and  $\mathbf{E}^k$  is the electric field intensity for the  $k^{th}$  layer. Integrating the electric field displacement vector over the effective area of the electrode surface we obtain the surface charge. In the case of a plate, it is assumed that for a piezoelectric layer acting as a sensor the electric field intensity is negligible. The eqn. (2) is thus simplified to,

$$D_3^k = \mathbf{e} \mathbf{e} \quad (3)$$

In finite element terms,

$$D_3^k = \mathbf{e} \mathbf{B} \mathbf{d}_e \quad (4)$$

Where,  $\mathbf{B}$  is the strain-displacement matrix and  $\mathbf{d}_e$  is the global displacement vector.

According to the Gauss law, the closed circuit charge measured through the electrodes of a sensor patch in  $k^{th}$  layer is,

$$q = \frac{1}{2} \left( \left[ \int_R D_3^k dA \right]_{z=z_k} + \left[ \int_R D_3^k dA \right]_{z=z_{k-1}} \right) \quad (5)$$

Where,  $R$  is the effective surface area of the piezoelectric patch. The effective area is the overlapping area of the electrode surfaces on both sides of the lamina. Substituting eqn. 4 in the above equation we get,

$$q = \int_R (\mathbf{e} \mathbf{B} \mathbf{d}_e) dA \quad (6)$$

#### ACTUATOR MECHANICS

The converse piezoelectric effect is expressed as,

$$\mathbf{s}_{ij} = \bar{\mathbf{D}} \mathbf{e}_{ij} - (\mathbf{e}^T \mathbf{E}_j) \quad (7)$$

Where,  $\bar{\mathbf{D}}$  is the matrix of elastic constants,  $\mathbf{E}_j$  is the electric field vector. The electric field vector is assumed to act across the thickness of the plate so that the electric field intensity is calculated as,

$$(E_3)^k = \frac{V^k}{h^k} \quad (8)$$

Where, the subscript 3 refers to the  $z$ -direction,  $h^k$  is the thickness of the  $k^{th}$  layer and  $V^k$  the voltage across the  $k^{th}$  layer. The equivalent actuator forces ( $N_x^p, N_y^p$  and  $N_{xy}^p$ ) and bending moments ( $M_x^p, M_y^p$  and  $M_{xy}^p$ ) are given as,

$$\begin{Bmatrix} N_x^p & M_x^p \\ N_y^p & M_y^p \\ N_{xy}^p & M_{xy}^p \end{Bmatrix} = \sum_{k=1}^{N_{lay}} \int_{z(k-1)}^{z(k)} \begin{Bmatrix} e_{31} \\ e_{32} \\ 0 \end{Bmatrix} (1, z) (E_3)^k dz \quad (9)$$

The nodal force vector is given as,

$$\mathbf{F}^p = \int \mathbf{B}^T \begin{Bmatrix} \mathbf{N}^p \\ \mathbf{M}^p \end{Bmatrix} dA \quad (10)$$

### 3. CONTROL ALGORITHM

A velocity feedback algorithm is employed in the present work. The charge ( $q$ ) developed on the sensor is differentiated with respect to time to obtain current. The current is amplified using a current amplifier and fed back to the actuators. The control forces generated by the actuators contribute to the velocity terms of eqn. 1. Therefore, the damping characteristics of the system are altered. The sensor voltage is calculated as,

$$V_s = \frac{dq}{dt} R \quad (11)$$

Where,  $R$  is the resistance of the piezoelectric material. The feedback voltage is,

$$V_a = G_i V_s = G \frac{dq}{dt} \quad (12)$$

Where,  $G_i$  is current amplifier gain and  $G$  is a combined coefficient representing the gain and the resistance of the piezoelectric material.

### 4. ENERGY CONSUMPTION

The apparent electrical power consumed by the piezoelectric actuator is given as,

$$P = V_a I \quad (13)$$

Where,  $V_a$  is the actuator input voltage and  $I$  is the current. As power is the time rate of energy, the

cumulative apparent electrical energy consumed ( $E_c$ ) is given by,

$$E_c = \int_T P \Delta t \quad (14)$$

The apparent electrical energy is the total electrical energy supplied to the system. In the present context, we define the cumulative apparent electrical energy in terms of an energy parameter ( $E_p$ ) given as,

$$E_p = \sum k V_a^2 \Delta t \quad (15)$$

Where,  $k$  is the coefficient that accounts for the actuator area and the resistance and  $\Delta t$  is the time step.

## 5. ACTUATOR SHAPE DESIGN

Under the influence of external excitation, the structure attains a deformed shape. The objective is to obtain the same deformed shape by efficient layout of the transducer. The deformed shape to be achieved is called as the *target* shape. When the two deformed profiles coincide exactly, the net deformation and therefore the sensed voltage in the structure would be zero. The cost functional to be minimized is the quadratic measure of the residual deviation of the current deformations of the structure from its target state. The objective function is thus defined as,

$$\min \left[ \int \{ \mathbf{d}_i(p_1, A_1, \dots, p_n, A_n) - \mathbf{d}_0 \}^2 dA \right] \quad (16)$$

Where,  $\mathbf{d}_i$  is the normalized deformation vector in  $i^{th}$  iteration, ( $A_1, \dots, A_n$ ) are the areas of actuators that are switched on, ( $p_1, \dots, p_n$ ) are the actuator position vectors and  $\mathbf{d}_0$  is the normalized target deformation vector (i.e. the mode shape). In dynamic control, a reciprocal relationship exists between a sensor and an actuator. That is, the shape of the actuator that excites a particular mode (modal actuator) is also the shape of the sensor that responds only to that mode (modal sensor). The present iterative procedure can therefore be employed in designing both, modal sensors as well as modal actuators.

A step-by-step procedure for transducer design is described below,

1. The structure is discretized into a fine finite element mesh. The eigenproblem is analyzed and the modal strains corresponding to the desired mode are obtained.
2. The shape design process begins with a maximal *seed* design wherein the entire domain is covered with transducer. Using sensor relation, the voltage in each element ( $V_s^e$ ) is calculated. It is to be noted that the transducer removal process involves switching off only the piezoelectric effect in the finite element corresponding to the candidate transducer location. This is termed as *transducer shading*.

To begin the process of removal of the actuators, a concept of *front opening* is introduced (fig. 1a).

```

Let, init = length of the stack
init=0;
do ielem=1, nelem
  if (ielem = element on the boundary)
    then
      init=init+1; ifron (init)=ielem !push
    end do
  end do

```

Only those transducers that surround the front are the candidates for state change (fig. 1b). The front progresses in both directions and the transducer profile gradually adapts to the shape that is most efficient in obtaining desired structural configuration. The front opening and subsequent removal of the transducers surrounding the front ensures that the final design that emerges is smooth and eliminates formation of such voids that could render its practical implementation difficult

3. Treating the current profile as an actuator, unit voltage is applied to the transducer pattern and the structure is reanalyzed in the presence of electrical effect only. Based on the deformations in the structure due to this electrical effect, the voltages developed at same locations (treating the transducer as a sensor) are calculated ( $V_a^e$ ).

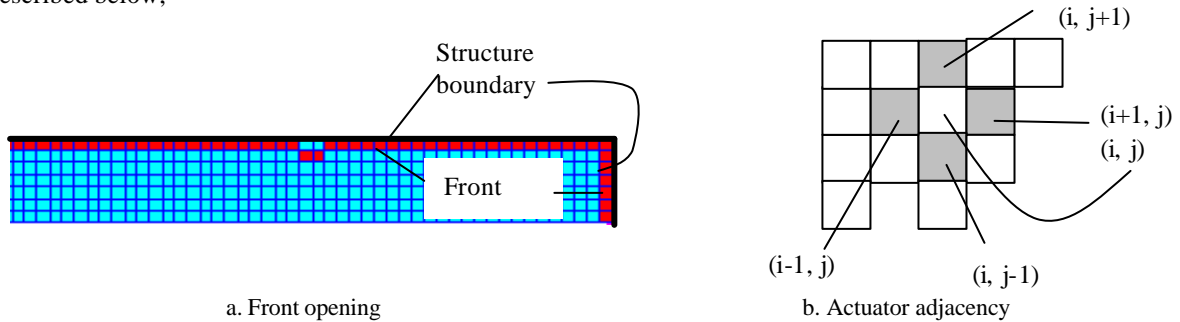


Figure 1: Front growth

4. The voltages  $V_a^e$  and  $V_s^e$  are normalized with respect to their maximum values.

$$\bar{V}_s^e = \frac{V_s^e}{(V_s^e)_{\max}}; \quad \bar{V}_a^e = \frac{V_a^e}{(V_a^e)_{\max}} \quad (17)$$

The residual voltages ( $V_r^e$ ) for the transducers on the front are determined as,

$$V_r^e = (\bar{V}_s^e - \bar{V}_a^e) \quad (18)$$

The locations that have negative residuals are potential candidates for removal.

```

iremov=0
do istack = 1, init
  if (Vr (ifron(istack)) < 0.0) then
    iremov=iremov+1
    nadd (iremov) = ifron(istack) ! potential
                                candidates
  end do

```

The candidate actuators are then ranked in the descending order based on the voltage residuals. A preset number of actuators are *popped out* of the stack.

5. The quadratic measure of the global residual deviation (**a**) in deformation is calculated as,

$$\mathbf{a} = \sum_{i=1}^{ndof} (\mathbf{d}_i - \mathbf{d}_0)^2 \quad (19)$$

The actuators adjacent to those selected for removal are *pushed into* the stack. In this way the front progresses in bidirectionally. In doing so, checks are applied to confirm that at new locations the actuators are not already removed and that the potentials are not already present in the stack. The new actuators occupy the positions in the stack that are freed due to removal of the current actuators. If any additional space is required, the stack length (*init*) is automatically increased.

6. Steps 3-5 are repeated till the value of **a** is acceptably small.

## 6. NUMERICAL EXAMPLE

**A simply supported rectangular plate subjected to air blast-** A rectangular graphite-epoxy plate (0.2m x 0.1m), simply supported at all four edges, is made up of three layers (0/90/0)

and a PVDF layer at the top and at the bottom. The constituent properties are given in table 1. It is subjected to blast pressure applied over the surface (fig. 2). Using symmetry only quarter plate is modeled with a 30 x 15 FE mesh and first two symmetric modes are obtained ( $f_1 = 269.93$  Hz and  $f_2 = 1214.76$  Hz). The transducer profile shown in fig. 3 is optimized for the fundamental mode using the algorithm outlined in the preceding section. The velocity feedback algorithm discussed in section 3 is employed in controlling the response of the plate. The frequency response (fig. 4) validates the efficacy of the two-dimensional shaped sensor in modal filtering. Owing to reciprocal relationship, the same design can be employed as a modal actuator.

The influence of the shape of the actuator on the response of the structure is investigated. The shapes considered are - actuator covering the entire surface of the structure (unweighted actuator) and the actuator shaped to excite the fundamental mode of the structure (fig. 3). The efficacy of the modal actuator over unweighted actuator is examined with the following objectives,

- a. Energy consumption for the same attenuation rate as that for the unweighted actuator.
- b. Attenuation rate for same energy characteristics as that for the unweighted actuator.

In the first case, the objective is to obtain a constant gain at which the modal actuator simulates the response of the unweighted actuator as closely as possible using lesser energy. To obtain this gain, a multiplying factor is calculated as a ratio of logarithmic decrements in case of the unweighted actuator and the modal actuator. For  $G = 5 \times 10^6$ , the multiplying factor based on the logarithmic decrements is 1.75. Therefore, the gain at which the modal actuator gives same attenuation rate as that of the unweighted actuator is  $8.75 \times 10^6$ . As seen from fig. 6 the modal actuator consumes about 20 % less energy to simulate the response of the unweighted actuator. It also indicates that for same energy consumption as that of the unweighted actuator the modal actuator would display improved attenuation characteristics, which is the second objective.

Table 1 Constituent Properties

Property	PVDF	Graphite-Epoxy
Young's Modulus (GPa), $E_1, E_2$	2.0, 2.0	150.0, 9.0
Poisson's Ratio, $\nu_{12}$	0.30	0.30
Shear Modulus (GPa), $G_{12}, G_{23}, G_{13}$	0.775	7.1, 2.5, 7.1
Piezoelectric constant, (C/m <sup>2</sup> ), $e_{31} = e_{32}$	-0.046	-
Thickness (mm) of lamina, Number of layers	0.50, 2	0.50, 3
Mass Density (N s/m <sup>4</sup> ), $\rho$	1800	1600

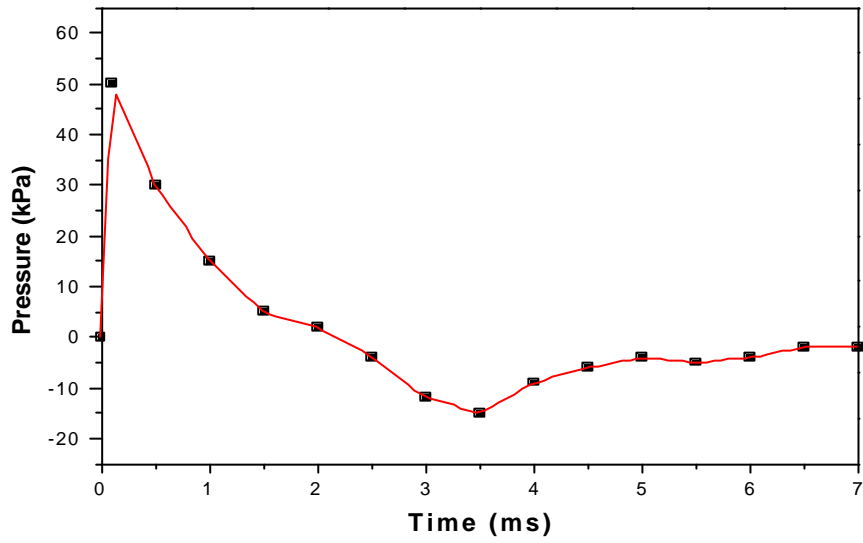


Figure 2 Air blast<sup>12</sup>

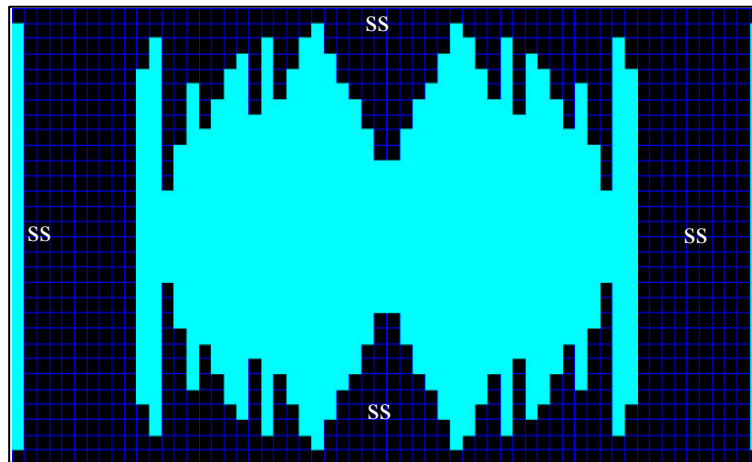


Figure 3 Sensor design optimized for the first mode.

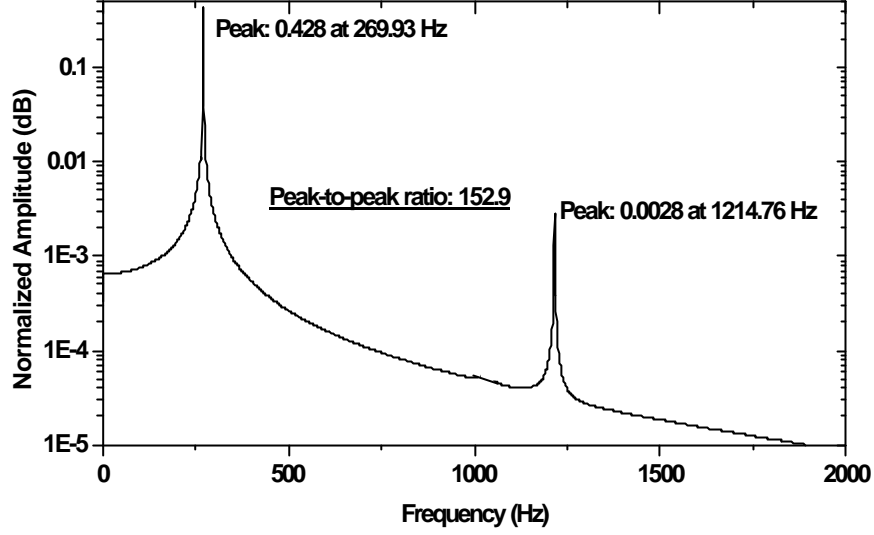


Figure 4 Response of mode-1 design to blast load.

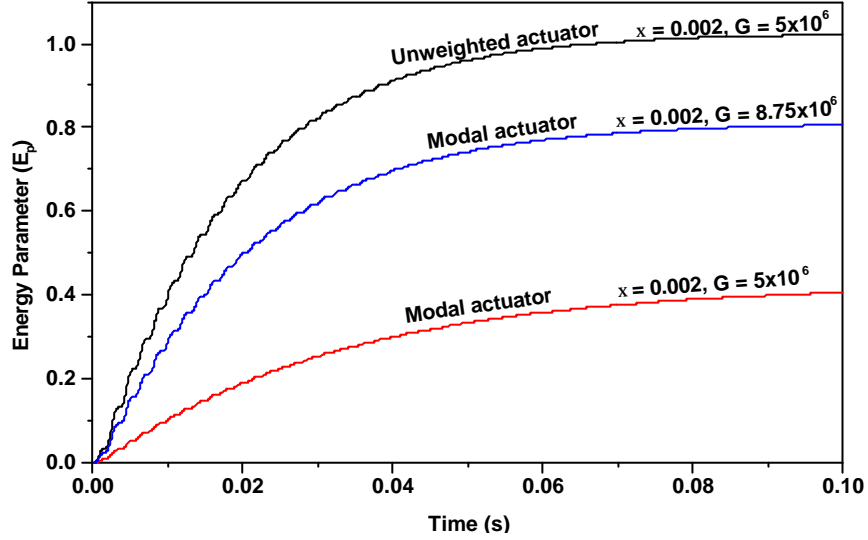


Figure 6: Cumulative energy consumption for unweighted and modal actuator for different gains.

In the second case, the gain is varied such that the cumulative energy consumed by the modal actuator at each time step is the same as in case of the unweighted actuator. Equating the energies in unweighted and modal actuator at each time step, the gain at each time step is given as,

$$G_{si} = \left[ \frac{\sum V_{fi} \sqrt{k_f}}{\sum V_{si} \sqrt{k_s}} \right] G_f \quad (22)$$

Where,

$G_{si}$  = Gain in modal actuator at  $i^{th}$  time step

$G_f$  = Gain in unweighted actuator

$k_s$  = Coefficient accounting for area and resistance of modal actuator

$k_f$  = Coefficient accounting for area and resistance for the unweighted actuator

$V_{si}$  = Sensed voltage in case of modal actuator at  $i^{th}$  time-step

$V_{fi}$  = Sensed voltage in case of unweighted actuator at  $i^{th}$  time-step

As seen in fig. 7 the modal actuator with variable gain shows improved response attenuation rate. The damping ratio in this case is about 15 percent higher than the unweighted actuator with constant gain. Thus, for the same energy consumption, the modal actuator with variable gain is a better performer than the unweighted actuator with constant gain.

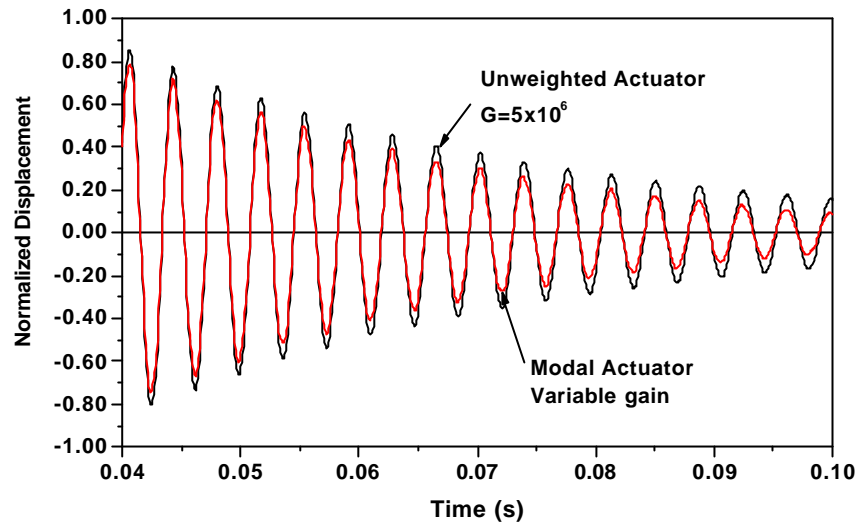


Figure 7 Comparison of the tip displacement responses using unweighted and modal actuator for same cumulative energy consumption.

## 7. CLOSING REMARKS

In this paper, the energy efficiency of a two-dimensional modal actuator has been demonstrated. The modal design is produced using the gradientless design optimization technique. The modal actuator possesses higher energy efficiency than the unweighted actuator as it consumes lesser energy to simulate the response by the unweighted actuator. Further, the modal actuator with variable gain shows improved response reduction than the unweighted actuator with constant gain for same energy consumption characteristics. These aspects are significant in practical situations in order to design energy efficient autonomous structures.

## REFERENCES

1. Fripp, M. L. and Atalla, M. J. "Review of modal sensing and actuation techniques", *The Shock and Vibration Digest*, **33** (1), 3-14, 2001
2. Meirovitch, L. *Dynamics and control of structures*. A Wiley-Interscience Publication. 1990.
3. Lee, C. -K. and Moon, F. C. "Modal sensors/actuators". *ASME Journal of Applied Mechanics*, **57**, 434-441, 1990.
4. Friswell, M. I. "On the design of modal actuators and sensors", *Journal of Sound and Vibration*, **241**, 361-372, 2001.
5. Mukherjee, A. and Joshi, S. P. "A gradientless technique for optimal distribution of piezoelectric material for structural control", *International Journal for Numerical Methods in Engineering*, **57**, 1737-1753, 2003.
6. Jordan, T., Ounaies, Z., Tripp, J. and Tchong, P. "Electrical properties and power considerations of a piezoelectric actuator" *NASA/CR-2000-209861*, 2000.
7. Brennan, M. C. and McGowan, A-M. "Piezoelectric power requirements for active vibration control", *Proceedings of SPIE: Smart Structures and Materials*, **3039**, 660-664, 1997.
8. Liang, C., Sun, F. P. and Rogers, C. A. "Determination of design of optimal actuator location and configuration based on actuator power factor", *Journal of Intelligent Material System and Structures*, **6**, 456-464. 1995.
9. Stein, S. C., Liang, C. and Rogers, C. A. "Power consumption of piezoelectric actuators driving a simply supported beam considering fluid coupling", *Journal of Acoustical Society of America*, **96**, 1598-1604, 1994.
10. Mukherjee, A. and Joshi, S. P. "Design of actuator profiles for minimum power consumption", *Smart Materials and Structures* **10**, 305-313. 2001.
11. Mukherjee, A. and Joshi, S.P. "Energy efficient actuators in vibration control of

- plated structures", *Journal of Sound and Vibration*, **258** (1), 179-190, 2002.
12. Houlston, R., Slater, J. E., Pegg, N. and Des Rochers, G.G. "On analysis of structural response of ship panels subjected to air blast loading", *Computers and Structures*, **21**, 273-289, 1985
13. Mukherjee, A. On finite element dynamic and stability analyses of stiffened plated structures, *PhD Thesis Indian Institute of Technology, Kharagpur*, 1987.